Scaling of convective mixing in porous media

Juan J. Hidalgo,[1,2] Jaime Fe,[3] Luis Cueto-Felgueroso,[1] and Ruben Juanes[1,*]

[1] *Massachusetts Institute of Technology, Cambridge, Massachusetts, USA*

[2] *Institute for Environmental Assessment and Water Research, Spanish National Research Council, Barcelona, Spain*

[3] *University of A Coruña, A Coruña, Spain*

(Dated: September 22, 2012)

Convective mixing in porous media is triggered by a Rayleigh–Bénard-type hydrodynamic instability as a result of an unstable density stratification of fluids. While convective mixing has been studied extensively, the fundamental behavior of the dissolution flux and its dependence on the system parameters are not yet well understood. Here, we show that the dissolution flux and the rate of fluid mixing are determined by the mean scalar dissipation rate. We use this theoretical result to provide computational evidence that the classical model of convective mixing in porous media exhibits, in the regime of high Rayleigh number, a dissolution flux that is constant and independent of the Rayleigh number. Our findings support the universal character of convective mixing and point to the need for alternative explanations for nonlinear scalings of the dissolution flux with the Rayleigh number, recently observed experimentally.

PACS numbers: 47.56.+r, 47.20.Bp, 92.40.K-

Convective mixing in porous media results from the density increase in an ambient fluid as solute or another fluid dissolves into it, leading to a Rayleigh–Bénard-type instability [1]. This phenomenon has received renewed attention because of its role in geologic carbon dioxide (CO_2) sequestration in saline aquifers [2]. When supercritical CO_2—which is less dense than brine—dissolves in brine, the aqueous mixture increases its density, leading to a configuration in which the dissolution of CO_2 is enhanced by the downward migration of dense fingers of CO_2-rich groundwater [3, 4], thereby accelerating solubility trapping of the injected CO_2 and increasing the security of storage [5]. Convective mixing may also play a role in the dissolution of halites or other soluble low-permeability rocks overlying groundwater aquifers [6], leading to high dissolution rates that can exert a powerful control on pore-water salinity in deep geologic formations [7]. Recent studies of convective mixing during CO_2 storage have addressed the stability analysis for the onset of convection [8–11], nonlinear simulation of the convective instability [9, 12–15], and experimental systems reproducing the conditions for convective mixing in a stationary horizontal layer [15–18].

The key dimensionless group in the problem is the Rayleigh number, Ra, which is a measure of the strength of density-driven convection relative to diffusion [1]. Experiments and high-resolution simulations suggest that, for high Ra, there exists a period of constant dissolution flux, after the onset of the instability and before the layer of brine starts to be saturated with dissolved CO_2 [12–14]. This constant-flux regime is crucial because it determines the importance of solubility trapping in geologic CO_2 sequestration [19].

The fundamental question of how this constant flux depends on Ra has been the subject of recent studies. Based on an argument of universality of the flow before it is affected by the boundaries [9, 11, 13, 18], the characteristic length of the problem is such that convection balances diffusion over that lengthscale, so one expects the constant dissolution flux during the convection-controlled regime to be independent of Ra; this is our null hypothesis. In contrast, recent experimental studies using a fluid system that naturally undergoes convection [15, 17] suggest a nonlinear scaling of dissolution flux with Ra. Thus, it is unclear how to reconcile these results and whether the origin of the observed nonlinear scaling can be explained from the classical mathematical model of porous-media convective mixing.

Here we investigate, by means of high-resolution numerical simulation, the scaling behavior of convective mixing for two model systems that have recently been investigated experimentally: (1) the canonical Rayleigh–Bénard–Darcy model problem with dissolution from the top boundary and linear dependence of density on the dissolved concentration [16, 18]; and (2) an analogue model for CO_2 sequestration in which a mixture of two miscible fluids exhibits a nonmonotonic density–concentration curve such that mixtures with intermediate concentrations are denser than either pure fluid [15, 17].

One of the inherent difficulties for the analysis of the analogue-fluid model (either from experiments or simulations) is finding a proper definition of the dissolution flux. While this is trivial for the canonical Rayleigh–Bénard–Darcy problem—where the dissolution flux can be obtained from the cumulative dissolved mass—it is a challenge for the analogue-fluid problem because there is no net accumulation of solute in the initial fluid: instead, two initially-segregated fluids mix through a one-sided instability. Here we resolve this challenge by deriving the relationship among diffusive flux, decay of concentration variance, and mean scalar dissipation rate. This relationship points to the scalar dissipation rate ϵ as the fundamental quantity that controls the evolution of convective mixing in either model system: any dependence on Ra must be reflected on ϵ.

We provide evidence that the classical mathematical model for single-phase variable-density flow in porous media under the Boussinesq approximation supports the null hypothesis that there is a universal regime in which the flux is constant and independent of Ra for both the canonical and analogue-

fluid systems. Therefore, deviations from this universal scaling must be due to factors not included in the mathematical model. We test whether they can be attributed to viscosity variations or to the shape of the density–concentration curve. We find that the scaling of the dissolution flux is relatively insensitive to variations in fluid viscosity, but depends strongly on the position of the maximum in the density–concentration curve. These findings could help reconcile some of the experimental observations.

Under the assumptions of incompressible fluids and the Boussinesq approximation, the governing equations for variable-density single-phase flow in a porous medium take the following dimensionless form [9]:

$$\begin{aligned} &\nabla \cdot \boldsymbol{u} = 0, \\ &\boldsymbol{u} = -\frac{1}{\mu(c)}(\nabla p - \rho(c)\hat{\boldsymbol{z}}), \\ &\partial_t c + \nabla \cdot \left(\boldsymbol{u}c - \frac{1}{\mathrm{Ra}}\nabla c\right) = 0, \end{aligned} \tag{1}$$

in $x \in [0, W]$ and $z \in [0, 1]$, where W is a dimensionless width. The first equation is the mass conservation equation for an incompressible fluid, where $\boldsymbol{u}$ is the dimensionless Darcy velocity. The second equation is Darcy's law, where p is the dimensionless pressure with respect to a hydrostatic datum, $\hat{\boldsymbol{z}}$ is the unit vector in the direction of gravity, ρ is a dimensionless density difference with respect to the initial fluid, and μ is a suitably rescaled dimensionless dynamic viscosity. The third equation is the advection-diffusion transport equation (ADE) for $c(x, z, t)$, the concentration rescaled between 0 and 1. The Rayleigh number Ra is the key dimensionless parameter of the problem:

$$\mathrm{Ra} = \frac{k\Delta\rho_\mathrm{m} g H}{\mu_\mathrm{m}\phi D_\mathrm{m}}, \tag{2}$$

where k is the aquifer permeability, ϕ is the porosity, $\Delta\rho_\mathrm{m}$ is the density difference driving convection, μ_m is the characteristic dynamic viscosity, D_m is the diffusion coefficient, and H is the height of the domain. In principle, both density and viscosity can be nonlinear functions of concentration.

In the canonical model, the density has a linear variation with concentration, so $\rho = c$. Moreover, the viscosity of the mixture is assumed to be constant, so $\mu = 1$. The initial condition is $c = 0$ everywhere in the domain. The boundary conditions are as follows: periodic boundary conditions in pressure and concentration at the lateral boundaries ($x = 0$, $x = W$); no-flow, no-diffusion at the bottom boundary ($z = 1$); and no-flow and prescribed concentration ($c = c_0 = 1$) at the top boundary ($z = 0$). Thus, along the top boundary, there is a dissolution flux from diffusion.

In the analogue-fluid model, the density is a nonlinear, non-monotonic function of concentration. The function $\rho(c)$ for the dimensionless density difference takes a value of 0 at $c = 0$, increases to a maximum value $\rho = 1$ at concentration $c = c_\mathrm{m}$ of the densest mixture, and decreases to a negative value at $c = 1$. Here, we use the density–concentration curve $\rho(c)$ for mixtures of propylene-glycol (PG) and water [17, 20], which we approximate by a polynomial that takes a maximum value at $c_\mathrm{m} = 0.26$. We also allow variations in the dynamic viscosity of the mixture, following an exponential law $\mu(c) = \exp(R(c_\mathrm{m} - c))$, where $R = \ln(\mu_0/\mu_1)$ is the viscosity ratio between the heavy and light fluids. The initial configuration is one in which the two pure fluids are segregated by density, with the lighter fluid on top ($c = 1$ for $0 \le z \le 0.1$) and the denser fluid below ($c = 0$ for $0.1 < z \le 1$). As the two fluids mix, initially by diffusion, a layer of dense fluid forms at the interface, triggering the convective-mixing instability. The boundary conditions are no-flow, no-diffusion at the top and bottom boundaries, and periodic boundary conditions at the side boundaries.

We consider first the canonical Rayleigh–Bénard–Darcy model of convective mixing driven by boundary-diffusion. We derive the evolution equations for the mean concentration $\langle c\rangle(t) = \int_\Omega c(x, z, t)\, d\Omega$ and the concentration variance $\sigma_c^2(t) = \int_\Omega [c(x, z, t) - \langle c\rangle(t)]^2\, d\Omega$ on the rectangular spatial domain (we have assumed, for expositional simplicity, a unit-square domain). The equation for the mean concentration is obtained by integrating the ADE:

$$\partial_t \langle c\rangle = F, \tag{3}$$

where $F = \int_{\Gamma_\mathrm{top}} \mathrm{Ra}^{-1}\nabla c \cdot \boldsymbol{n}\, d\Gamma$ is the integrated diffusive flux across the top boundary ($z = 0$). The equation for the concentration variance is obtained by multiplying the ADE by c and integrating over the domain. Incorporating the incompressibility constraint, the boundary conditions, and after some algebraic manipulations, one obtains:

$$\partial_t \sigma_c^2 = 2(c_0 - \langle c\rangle)F - 2\langle\epsilon\rangle, \tag{4}$$

where $c_0 = 1$ is the prescribed concentration at the top boundary, and $\epsilon = \nabla c \cdot \mathrm{Ra}^{-1}\nabla c$ is the scalar dissipation rate [21]. The central role of the scalar dissipation rate has been exploited recently to explain anomalous fluid mixing in porous media driven by permeability heterogeneity [22] or viscous-fingering instabilities [23]. Equation (4) exposes the fundamental relationship among mixing rate, dissolution flux and mean scalar dissipation rate, and makes it evident that any Rayleigh-number dependence of the dissolution flux F must be reflected also in the mean scalar dissipation rate $\langle\epsilon\rangle$.

The link to the scalar dissipation rate is particularly useful to characterize the time evolution in the analogue-fluid model. In this case, there is no proper dissolution flux but, rather, a convection-dominated mixing of the two initial miscible fluids. Since all boundaries are no-flux boundaries, the mean concentration $\langle c\rangle$ is constant, and the concentration variance equation reduces to:

$$\partial_t \sigma_c^2 = -2\langle\epsilon\rangle. \tag{5}$$

Analyzing $\langle\epsilon\rangle$ provides a fundamentally new way to characterize the macroscopic evolution of convective mixing, and a rigorous way to quantify any dependence on Ra.

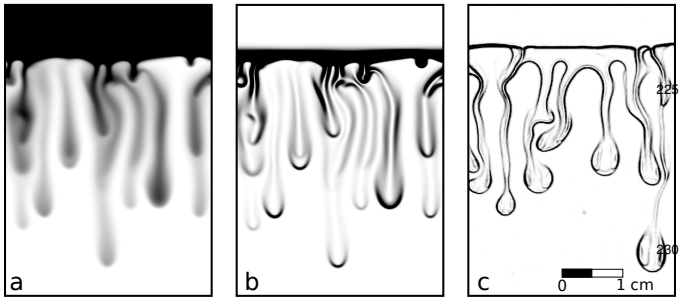

FIG. 1. **a,** Snapshot of the concentration c at dimensionless time $t = 1$ from a simulation of the analogue-fluid system with $\mathrm{Ra} = 10,000$ and constant viscosity ($R = 0$). A computational grid of 512×1536 cells was used, and only a small window of the simulation domain is shown. **b,** Corresponding snapshot of the scalar dissipation rate ϵ, for the same simulation as that in figure a. Here, dark color corresponds to high values of ϵ, and indicates regions of active mixing. **c,** Snapshot of a surrogate of the scalar dissipation rate $\epsilon = \nabla c \cdot D_m \nabla c$ (obtained from light intensity) from a laboratory experiment with a PG–water system in a Hele-Shaw cell, illustrating that mixing is primarily confined to narrow layers along the edges of the horizontal interface and the density-driven fingers.

We perform high-resolution computer simulations of the governing equations (1), for both the canonical model and the analogue-fluid model. We employ the so-called streamfunction–vorticity formulation, in which the equation for the streamfunction and the ADE transport equation are solved sequentially at each time step [24]. We solve the streamfunction equation using a spectral method [9, 25], and the concentration equation using a sixth-order compact finite difference discretization and a third-order Runge-Kutta time-stepping scheme [24]. We trigger the density-driven instability by introducing a small perturbation on the concentration at the boundary (for the canonical system) or the horizontal initial interface (for the analogue-fluid system), as it is commonly done [9, 14, 15].

The results of a typical simulation are shown in Fig. 1. The morphology of the convective instability is well known [9, 15, 17, 18]: after an onset period in which a diffusion layer builds up between the two fluids, the layer develops a one-sided instability in which downward-moving protrusions grow exponentially, eventually developing into blob-like fingers with thin necks at the roots of the fingers; these fingers then interact, merging into each other, and coarsening in such a way that well-developed fingers then attract newly formed fingers (Fig. 1a). A snapshot of the simulated scalar dissipation rate ϵ illustrates that the regions where the fluids are actively mixing coincide with the edges of the density-driven fingers (Fig. 1b). This behavior is supported qualitatively by laboratory experiments with a PG–water system in an Hele-Shaw cell (Fig. 1c).

In Fig. 2 we plot the time evolution of the mean scalar dissipation rate for both the canonical Rayleigh–Bénard–Darcy model and the analogue-fluid model, and for different values of Ra. For each case, there is a regime of constant rate of scalar dissipation. That period extends, roughly, from dimensionless time $t = 1$ to $t = 6$, which is about twice the time that it takes for the fingers to reach the bottom of the domain, indeed highlighting the convective nature of the dissolution process. It is interesting that the scalar dissipation rate for the boundary-driven dissolution case is approximately twice as large as that for the analogue-fluid model, in analogy with the diffusive flux for one-dimensional diffusion from a one-sided boundary problem vs. two-sided diffusion from an initial sharp discontinuity.

We compute the time-averaged mean scalar dissipation rate, $\overline{\langle\epsilon\rangle}$, during the time period of constant dissolution flux ($t \in [1, 6]$ for the canonical model and $t \in [2, 8]$ for the analogue-fluid model). For simulations with high Ra (> 5000), the scalar dissipation rate appears to be independent of Ra (Fig. 2, inset). Given the fluctuations of the mean scalar dissipation rate over time, one cannot reject the null hypothesis that the dissolution flux is independent of the Rayleigh number. Indeed, we fit a power law to $\overline{\langle\epsilon\rangle}$ obtained from the high-resolution simulations as a function of Ra. This yields a best fit (with 95% confidence bounds) $\overline{\langle\epsilon\rangle} \approx (0.0120 \pm 0.0013)\mathrm{Ra}^{+0.031\pm0.012}$ for the canonical model, and $\overline{\langle\epsilon\rangle} \approx (0.0072 \pm 0.0012)\mathrm{Ra}^{-0.017\pm0.017}$ for the analogue-fluid model. These results provide conclusive evidence that the classical Darcy–Boussinesq model of convective mixing predicts a regime in which the dissolution flux and subsequent mixing is constant and, in the range of high Ra, independent of the Rayleigh number.

However, recent experimental studies using analogue fluids, like methanol–ethylene glycol and water (MEG–water) [15] and propylene glycol and water (PG–water) [17], report a scaling of the form $F \sim \mathrm{Ra}^{-1/5}$. Here, we explore the possibility that this nonlinear scaling be due to the viscosity contrast between the fluids or to the shape of the density–concentration curve.

To investigate the effect of viscosity contrast between the pure fluids, we perform simulations of the analogue-fluid model with a range of values of the log-viscosity ratio R, from -2 to 2. A positive value of R means that the lighter fluid is less viscous, which is the case for the PG–water system (water is less dense and less viscous). The time-averaged scalar dissipation rate exhibits a weak dependence on the viscosity contrast, such that there is a natural ordering in which the mixing rate is larger for lower values of R. For a fixed value of R, there is no clear dependence of $\overline{\langle\epsilon\rangle}$ on Ra (Fig. 3).

To investigate the effect of the shape of the density–concentration curve, we perform simulations using a simple parameterization of the density curve. It is assumed to be a continuous piecewise linear function with the same endpoints as that of the PG–water system, $\rho(0) = 0$ and $\rho(1) = -3.6$, connected with the point at which the density is maximum, $\rho(c_\mathrm{m}) = 1$. We then study the influence of c_m, which we vary between 0.1 and 0.8, and find that the mixing rate exhibits a strong monotonic dependence on the position of the maximum density: larger values of c_m lead to larger mixing rates

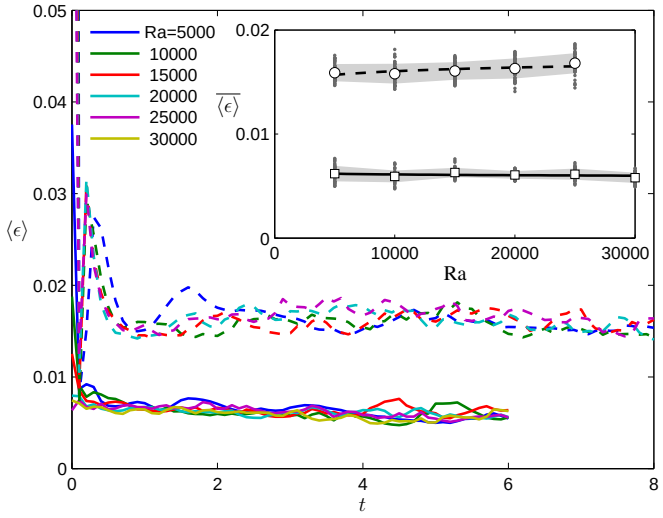

FIG. 2. Time evolution of the mean scalar dissipation rate $\langle\epsilon\rangle$ from simulations of both the canonical Rayleigh–Bénard–Darcy model (dashed lines) and the analogue-fluid model (solid lines). We report results for different Rayleigh numbers varying from $\mathrm{Ra} = 5000$ to $30,000$, and constant viscosity ($R = 0$). All cases exhibit a period of constant rate of scalar dissipation. For each model, all the curves seem to collapse, suggesting weak or no dependence on Ra. **Inset:** Time-averaged scalar dissipation rate for the canonical model (circles) and the analogue-fluid model (squares). For each Ra, the small dots denote the entire time series of $\langle\epsilon\rangle$ ($t \in [1, 6]$ for the canonical model and $t \in [2, 8]$ for the analogue-fluid model, at time intervals of $\delta t = 0.1$). The shaded areas indicate the spread of one standard deviation with respect to the average. We indicate, with a line, the best power-law fit over all simulations for each case. The best fit is virtually independent of Ra.

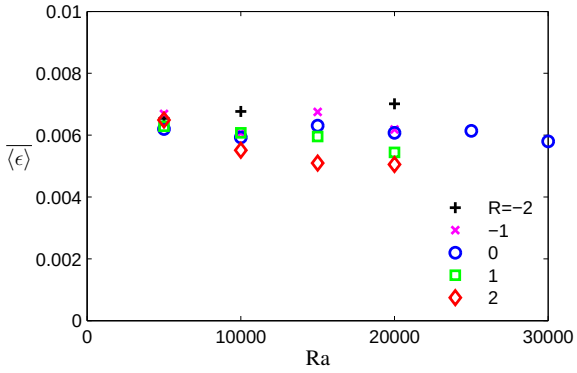

FIG. 3. Impact of viscosity variations on the time-averaged mean scalar dissipation rate $\overline{\langle\epsilon\rangle}$. All simulations are for the analogue-fluid system with different values of log-viscosity ratio ($R = -2$ to 2). For each value of R, we plot $\overline{\langle\epsilon\rangle}$ as a function of Ra.

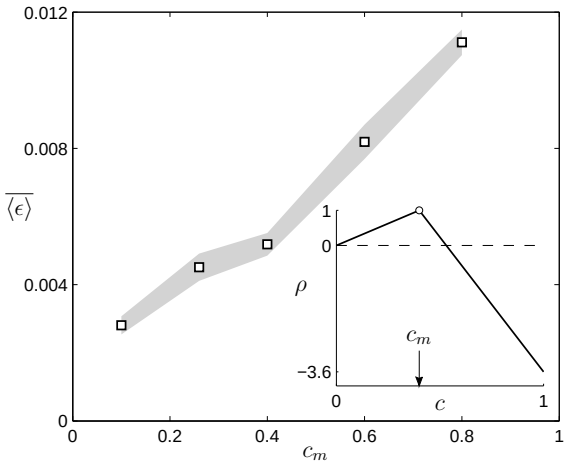

FIG. 4. Impact of the shape of the density–concentration curve on the time-averaged mean scalar dissipation rate $\overline{\langle\epsilon\rangle}$. We fix the value of the Rayleigh number ($\mathrm{Ra} = 20,000$) and use constant viscosity ($R = 0$), and run simulations for different piecewise-linear density curves, parameterized by the concentration c_m at which the curve takes its maximum value (see inset).

(Fig. 4).

In summary, we have shown that in the problem of dissolution-driven convection in porous media, any dependence of the dissolution flux on the Rayleigh number must translate into a dependence of the scalar dissipation rate on Ra as well. This observation is essential to interpret the simulations of an analogue fluid-mixture model in which several recent experiments are based. Our high-resolution simulations of convective mixing show that the classical Darcy–Boussinesq equations of variable-density flow in porous media lead to mean scalar dissipation rates that are independent of Ra. Therefore, nonlinear scalings of dissolution flux with Ra must be explained by effects that are not present in the traditional Darcy–Boussinesq model equations of convective mixing. Here, we have analyzed the effects of viscosity variations and the shape of the density curve. While the predicted mixing rates depend only weakly on the viscosity contrast between the pure fluids, they depend strongly on the shape of the density–concentration curve and, in particular, on the position of the maximum of the curve. These effects, along with others not investigated here such as volume change on mixing [26], could help reconcile the Rayleigh-number dependence observed experimentally [15, 17].

We thank Christopher MacMinn and Michael Szulczewski for comments. JJH acknowledges the support from the FP7 Marie Curie Actions of the European Commission, via the CO2-MATE project (PIOF-GA-2009-253678). RJ acknowledges funding by the Cooperative Agreement Between the Masdar Institute of Science and Technology (Masdar Institute), Abu Dhabi, UAE and the Massachusetts Institute of Technology (MIT), Cambridge, MA, USA, Reference No. 196F/002/707/102f/70/9374.

* juanes@mit.edu

[1] D. A. Nield and A. Bejan, *Convection in Porous Media*

(Springer, New York, 2006).
[2] IPCC, *Special Report on Carbon Dioxide Capture and Storage,* B. Metz et al. (eds.) (Cambridge University Press, 2005).
[3] E. Lindeberg and D. Wessel-Berg, Energy Conv. Manag. **38**, S229 (1997).
[4] J. Ennis-King and L. Paterson, Soc. Pet. Eng. J. **10**, 349 (2005).
[5] M. L. Szulczewski, C. W. MacMinn, H. J. Herzog, and R. Juanes, Proc. Natl. Acad. Sci. U.S.A. **109**, 5185 (2012).
[6] R. L. Van Dam, C. T. Simmons, D. W. Hyndman, and W. W. Wood, Geophys. Res. Lett. **36**, L11403 (2009).
[7] G. Garven, Annu. Rev. Earth Planet. Sci. **89**, 89 (1995).
[8] J. Ennis-King, I. Preston, and L. Paterson, Phys. Fluids **17**, 084107 (2005).
[9] A. Riaz, M. Hesse, H. A. Tchelepi, and F. M. Orr, Jr., J. Fluid Mech. **548**, 87 (2006).
[10] S. Rapaka, S. Chen, R. J. Pawar, P. H. Stauffer, and D. Zhang, J. Fluid Mech. **609**, 285 (2008).
[11] A. Slim and T. S. Ramakrishnan, Phys. Fluids **22**, 124103 (2010).
[12] H. Hassanzadeh, M. Pooladi-Darvish, and D. W. Keith, AIChE J. **53**, 1121 (2007).
[13] J. J. Hidalgo and J. Carrera, J. Fluid Mech. **640**, 441 (2009).
[14] G. S. H. Pau, J. B. Bell, K. Pruess, A. S. Almgren, M. J. Lijewski, and K. Zhang, Adv. Water Resour. **33**, 443 (2010).
[15] J. A. Neufeld, M. A. Hesse, A. Riaz, M. A. Hallworth, H. A. Tchelepi, and H. E. Huppert, Geophys. Res. Lett. **37**, L22404 (2010).
[16] T. J. Kneafsey and K. Pruess, Transp. Porous Media **82**, 123 (2010).
[17] S. Backhaus, K. Turitsyn, and R. E. Ecke, Phys. Rev. Lett. **106**, 104501 (2011).
[18] A. Slim, M. M. Bandi, J. C. Miller, and L. Mahadevan, Phys. Fluids (2012), to be published.
[19] C. W. MacMinn, M. L. Szulczewski, and R. Juanes, J. Fluid Mech. **688**, 321 (2011).
[20] Dow Chemical, "Propylene glycols - density values," (2011), https://dow-answer.custhelp.com/app/answers/detail/a_id/7471.
[21] S. B. Pope, *Turbulent Flows* (Cambridge University Press, 2000).
[22] T. Le Borgne, M. Dentz, D. Bolster, J. Carrera, J.-R. de Dreuzy, and P. Davy, Adv. Water Resour. **33**, 1468 (2010).
[23] B. Jha, L. Cueto-Felgueroso, and R. Juanes, Phys. Rev. Lett. **106**, 194502 (2011).
[24] M. Ruith and E. Meiburg, J. Fluid Mech. **420**, 225 (2000).
[25] C. T. Tan and G. M. Homsy, Phys. Fluids **6**, 1330 (1988).
[26] F. M. Orr, Jr., *Theory of Gas Injection Processes* (Tie-Line Publications, Copenhagen, 2007).